

Evaluatoin of Incompressible and Compressible SPH Methods in Modeling Dam Break Flows

Hassan Akbari¹

¹ Assistant Professor at Tarbiat Modares University, Tehran, Iran, h.akbari@modares.ac.ir

ARTICLE INFO

Article History:

Received: 27 Nov. 2017

Accepted: 15 Jun. 2018

Keywords:

ISPH

WCSPH

Accuracy

Stability

free surface boundary

ABSTRACT

Smoothed Particle Hydrodynamic (SPH) is an attractive Lagrangian tool for simulating flows with large displacement at free surface boundary. Two widely used subcategories of this method are Weakly compressible SPH (WCSPH) and truly Incompressible SPH (ISPH) methods. Each method has its individual advantages while there is not yet a global agreement about the preference of one method to another one. In this study, accuracy, stability and efficiency of these methods are compared in simulating dam break flow as a well-known hydraulic problem. To decrease unrealistic particle fluctuation especially at free surface boundary, a practical solution is applied to both methods while keeping their total accuracy. In addition, different solid boundary treatments are studied and their effect on total accuracy and stability of SPH methods are investigated.

Based on the results, both ISPH and WCSPH methods can model free surface profiles properly if a proper solid boundary treatment is utilized. Meanwhile, local surface fluctuations can be damped in both methods efficiently by means of the modified surface viscosity.

By means of original versions, it is concluded that ISPH method is generally more stable and more accurate particularly in modeling pressure field than WCSPH method. In addition, it is shown that ISPH method is faster than WCSPH method in solving a dam break flow with equal number of particles. On the other hand, ISPH in its original version using the divergence-free velocity scheme suffers from density loss problem. Since a lot of modifications have been introduced till now to overcome defections of both methods, it is not fair to compare methods with different modifications and therefore, similar modifications are applied in this study. Meanwhile, it can be concluded that each method is growing and is going its own way through enhancement.

1. Introduction

The Smoothed Particle Hydrodynamics (SPH) method is a particle method in Lagrangian coordinate that was originally introduced for the astrophysics by Monaghan (1992). Large deformations at free surface boundaries can be modeled efficiently by Lagrangian particle approaches and contrary to the Eulerian grid approaches, no numerical diffusion occurs in Lagrangian methods due to solving advection term directly. In addition, free surface profile can be easily traced via this method. At first, Weakly Compressible SPH (WCSPH) method applied to the fluid mechanics by Monaghan and Kos (1999) and later, Incompressible SPH (ISPH) method introduced by Shao and Lo (2003) based on a semi-implicit

projection method. Gomez-Gesteira et al. (2010a) present the state-of-the-art of classical SPH for free surface flows and examined some improvement methods to classical SPH, especially for dam break problems. In WCSPH method, fluid is assumed compressible while incompressibility is ensured by means of pressure adjustment via equation of state. Lee et al. (2008) showed the efficiency of ISPH method particularly in improving the pressure field in comparison with WCSPH method. Later, several attempts have been made to improve the accuracy and functionality of ISPH method. Khayyer et al. (2008) revised the gradient of kernel function to improve the preservation of angular momentum. Xu et al. (2009) introduced a more stable method based on moving the

particles at the end of each time step through the streamlines and Rafiee et al. (2012) used modified Riemann solver to improve the accuracy of SPH methods.

To overcome unrealistic pressure oscillation in WCSPH methods, several attempts have been done such as density reinitializing, iteration or grid scheme methods (Monaghan 1989, Colagrossi and Landrini 2003, Fatehi and Manzari 2012, Violeau and Rogers 2016, Sun et al. 2017). However, this problem can be solved by means of ISPH method too.

Khayyer and Gotoh (2010b) modeled dam break flow using different modified forms of SPH, WCSPH and moving particle semi-implicit (MPS) methods. They concluded that the improved versions of these particle methods outperform the original versions in terms of both free surface profile and pressure field. According to their results, the WCSPH method modified using a moving least square (MLS) density re-initialization technique results in smoother pressure field than the modified MPS method. However, a distinctive disadvantage of WCSPH method in comparison with two other methods is that WCSPH methods need calibration constants. Khayyer and Gotoh (2010b) showed the importance of selecting a proper artificial viscosity in WCSPH methods. Later, Szwec et al. (2012) compared ISPH and WCSPH through simulating lid-driven cavity flow. They neglected the stability of pressure term and concluded that WCSPH needs more computational cost while density error accumulation occurs in the original forms of ISPH methods. However, the mentioned errors can be removed by means of relaxation coefficient or imposing additional viscosities (Lee et al. 2008, Xu et al. 2009, Asai et al. 2012, Akbari, 2017). Using higher orders Poisson Pressure Equation (PPE) or particle shifting can also improve the results of ISPH (Khayyer et al. 2017, Khayyer and Gotoh 2010a). Although ISPH method are concluded to be more efficient than WCSPH method in some of the studies (Lee et al. 2008, Lee et al. 2010, Gotoh and Khayyer, 2016), there is not yet a global agreement about this issue. Hughes and Graham (2010) by simulating dam break and wave impact on vertical wall concluded that in the optimum configuration, WCSPH could perform as well as ISPH and even in some respects better than ISPH. There is a similar conclusion in Shadloo et al.'s (2012) study where the accuracy of WCSPH method is mentioned as reliable as those of the ISPH and FEM. In addition, by comparing the numerical results with laboratory data corresponding to dam breaking flow, Lee et al. (2008) reported more unreliable fluctuations at the surface boundary in the case of utilizing ISPH method than WCSPH method. Meanwhile, Akbari (2017) introduced an efficient method that is applicable in both WCSPH and ISPH methods to control these unrealistic fluctuations at free surface profile. Gomez-Gesteira et al. (2010b)

reported these ongoing debates among the SPH community about the different approaches to treat the compressibility of the fluid and proves that additional research should be conducted to elucidate the pros and cons of the different approaches.

In this study, performance of ISPH and WCSPH methods in modeling a well-known dam break flow is studied and it is tried to clarify the main reasons of different conclusions in literatures. In next sections, after presenting basic equations and numerical issues, different numerical concerns including accuracy, stability, boundary conditions and computational cost of both ISPH and WCSPH methods are investigated and reported separately. Then, the main outcomes are summarized in conclusion part.

2. Governing Equations and Numerical models

2.1. Governing Equations

The well-known continuity equations for fluids are:

$$\frac{1}{\rho_w} \frac{D\rho_w}{Dt} + \nabla \cdot \vec{U}_f = 0 \quad (1)$$

$$\vec{\nabla} \cdot \vec{U}_f = 0 \quad (2)$$

Where, ρ_w and \vec{U}_f are density and velocity of the fluid, respectively. For a turbulent viscous flow, the Lagrangian format of momentum equation is:

$$\frac{D\vec{U}_f}{Dt} = \frac{-1}{\rho_w} \vec{\nabla} P + \nu_E \nabla^2 \vec{U}_f + \vec{g} \quad (3)$$

Where, P and \vec{g} represent total flow pressure and gravitational acceleration vector, respectively. Terms on the right hand side of Eq. (3) represents the pressure force caused by the pressure gradient, the viscous force and the gravitational acceleration, respectively. The effective viscosity $\nu_E = \nu_w + \nu_T$ is summation of fluid kinematic viscosity ν_w (1.0 E-6 for water) and Smagorinsky turbulent viscosity ν_T .

2.2. WCSPH and ISPH: Explicit and Semi-implicit methods

In WCSPH method, little compressibility is applied on the fluid via equation of state such as one proposed by Monaghan (1994) to calculate the pressure term:

$$P = \frac{\rho_w V_s^2}{7} \left(\left(\frac{\rho}{\rho_w} \right)^7 - 1 \right) \quad (4)$$

Where ρ and ρ_w are computed and reference fluid density, respectively. V_s is the sound velocity normally taken as ten times the maximum fluid velocity as reported by Lee et al. 2008 to limit the density variation to one percent. Because of the large speed of the sound and implemented power coefficient in Eq. (4), a small fluctuation in the density generate a large pressure between two

adjacent particles and keep them away. Then, the particle velocity in the next time step (n+1) can be calculated explicitly based on the forces from the previous time step (n) i.e. F^n and the selected time step Δt as:

$$\begin{aligned}\vec{U}_f^{n+1} &= \vec{U}_f^n + F^n \cdot \Delta t; \\ F^n &= \frac{-1}{\rho_w} \vec{\nabla} P^n + \nu_E \nabla^2 \vec{U}_f^n + \vec{g}\end{aligned}\quad (5)$$

The predictor corrector time stepping method is applied in this study for WCSPH method.

On the other hand, in the ISPH method, fluid incompressibility is imposed by means of semi-implicit projection method as introduced by Shao and Lo (2003). Density invariant (DI) method and divergence-free velocity (DV) method are two main categories of the projection methods. Xu et al. (2009) reported that DV method is more accurate than DI method as utilized in this study. In this method, an intermediate velocity \vec{U}_f^* is used and the momentum equation is written in two equations their summation generates the complete form of the momentum equation.

$$\frac{\vec{U}_f^* - \vec{U}_f^n}{\Delta t} = \nu_E \nabla^2 \vec{U}_f^n + \vec{g} \quad (6)$$

$$\frac{\vec{U}_f^{n+1} - \vec{U}_f^*}{\Delta t} = \frac{-1}{\rho_w} \vec{\nabla} P \quad (7)$$

By means of Eq. (6), intermediate velocity is obtained explicitly as:

$$\vec{U}_f^* = \vec{U}_f^n + \Delta t \times [\nu_E \nabla^2 \vec{U}_f^n + \vec{g}]^n \quad (8)$$

After Applying the divergence operator on both sides of Eq. (7) and considering a free divergence criterion ($\vec{\nabla} \cdot \vec{U}_f^{n+1} = 0$), the unknown pressure term at the next time step (P^{n+1}) can be obtained by solving the obtained system of linear equations as:

$$\frac{\vec{\nabla} \cdot \vec{U}_f^*}{\Delta t} = \vec{\nabla} \cdot \left(\frac{1}{\rho_w} \vec{\nabla} P^{n+1} \right) \quad (9)$$

This system is solved in this study by means of the Preconditioned Bi-conjugate Gradient Stabilized Method with Jacobi pre-conditioner as an iterative method with the converged normalized residual as 0.01. Then, the particle velocity is obtained simply by:

$$\vec{U}_f^{n+1} = \vec{U}_f^* - \Delta t \times \left[\frac{1}{\rho_w} \vec{\nabla} P^{n+1} \right] \quad (10)$$

After computing the velocity of particles at the new time step (by means of WCSPH or ISPH), each particle moves to its new position (\vec{r}^{n+1}) by making use of the averaged velocity as:

$$\vec{r}^{n+1} = \vec{r}^n + \frac{(\vec{U}_f^{n+1} + \vec{U}_f^n)}{2} \Delta t \quad (11)$$

2.3. SPH principles

In SPH method, each arbitrary function $f(x)$ is estimated at particle i by

$$f(x_i) = f_i \approx \sum_j f(x_j) W_{ij} V_j; V_j = \frac{m_j}{\rho_j} \quad (12)$$

Where, j denotes neighboring particles and W_{ij} is the value of kernel function of particle i at the position of particle j . Supporting domain of each particle is a function of smoothing length (h) of the kernel function. Selection of smoothing length is important. Large values increase the computational cost and increase the smoothing effects on the results. On the other hand, small values of this parameter may results in numerical instabilities due to no interaction between two adjacent particles. In this study, the effect of this parameter is studied and its default value is selected as 1.2 times of particle spacing according to other studies (Shao 2010, Khayyer et al. 2008, Price 2012). In this study, cubic B-Spline kernel function with dominant error of $O(h^2)$ in integral interpolant is used as proposed by Monaghan (1992). In SPH methods, the computational domain is divided to several particles and each particle i represents a mass of m_i and occupies a volume of V_i . Density of the fluid at that particle is ρ_i and is obtained based on the concentration of its neighbor particles j by means of density summation method i.e.

$$\rho_i = \sum_j m_j W_{ij} \quad (13)$$

Or, by making use of density variation method which is based on the mass continuity equation in WCSPH method:

$$\frac{D\rho_i}{Dt} = \sum_{j \neq i} m_j (\vec{u}_{ij} \cdot \vec{\nabla}_i W_{ij}) \quad (14)$$

In this equation, gradient of kernel function taken with respect to the particle i ($\vec{\nabla}_i W_{ij}$) is used and $\vec{u}_{ij} = \vec{U}_{fi} - \vec{U}_{fj}$ where \vec{U}_{fi} and \vec{U}_{fj} are particle velocities. Based on SPH algorithm, pressure gradient and velocity divergence is estimated as (Monaghan, 1992):

$$\vec{\nabla} P_i = \rho_i \sum_{j \neq i} m_j \left(\frac{p_i}{\rho_i^2} + \frac{p_j}{\rho_j^2} \right) \vec{\nabla}_i W_{ij} \quad (15)$$

$$\vec{\nabla} \cdot \vec{U}_f^* = \sum_{j \neq i} V_j (\vec{U}_{fj}^* - \vec{U}_{fi}^*) \cdot \vec{\nabla}_i W_{ij} \quad (16)$$

Where \vec{U}_{fi}^* and \vec{U}_{fj}^* are intermediate velocities at particle i and j , respectively. Viscosity term can be estimated by combining the first derivative of SPH and FDM methods as discussed by Shao and Lo (2003):

$$(\nu_E \nabla^2 \vec{U}_f)_i = \sum_{j \neq i} m_j \frac{2(\nu_{Ei} + \nu_{Ej})}{\rho_i + \rho_j} \cdot \frac{\vec{\nabla}_i W_{ij} \cdot \vec{r}_{ij}}{|\vec{r}_{ij}|^2 + \eta^2} \vec{u}_{ij} \quad (17)$$

In this equation, $\vec{r}_{ij} = \vec{r}_i - \vec{r}_j$ where \vec{r}_i and \vec{r}_j are the position vectors of the particles and $\eta = 0.1h$ as proposed by Lee et al. (2008). ν_{Ei} and ν_{Ej} are effective viscosity of particle i and j , respectively. Similarly, the pressure gradient can be estimated as:

$$\vec{\nabla} \cdot \left(\frac{1}{\rho_w} \vec{\nabla} P \right)_i = \sum_{j \neq i} m_j \frac{8}{(\rho_i + \rho_j)^2} \cdot \frac{\vec{\nabla}_i W_{ij} \cdot \vec{r}_{ij}}{|\vec{r}_{ij}|^2 + \eta^2} p_{ij} \quad (18)$$

Where, $p_{ij} = P_i - P_j$. Eq. (18) is actually the discrete form of Eq.(9) and therefore, it is not applicable in WSPH method where the pressure is obtained using the equation of state instead of solving the presented system of linear equations. On the other hand, angular momentum is not preserved in the common SPH method. However, this problem can be solved by correcting the kernel gradient via applying a corrective matrix \hat{L}_i as introduced by Bonet and Lok (1999). Khayyer et al. (2008) extended this improvement into SPH method and concluded that any linear velocity field gradient would be exactly evaluated via employment of the corrected kernel function as:

$$\tilde{\nabla}_i W_{ij} = \left(\sum_j V_j \vec{\nabla}_i W_{ij} \otimes (\vec{r}_j - \vec{r}_i) \right)_i \cdot \vec{\nabla}_i W_{ij} \quad (19)$$

This correction factor is applied on the kernel gradient in this study for both WSPH and ISPH methods to improve the accuracy of the equation discretization.

2.4. Tensile instability, artificial and surface viscosity

Tensile instability is one of the difficulties of the standard SPH where the particles attract each other and make unrealistic clumps when the fluid is compressed. Swegle et al. (1995) defined the criteria of this instability based on the negative pressure and the sign of the second derivative of the interpolating kernel. As a result, if distance between to pair particles gets closer than $2h/3$ in the case of using Cubic-Spline kernel function that is used in this study, these particles attract each other and perform a tensile instability. Dehnen and Aly (2012) reported less instability in the case of implementing Wendland kernel function. In addition, Monaghan (2000) suggested that the SPH tensile instability can be

removed by implementing a small repulsive term between the SPH particles and this solution is used in this study for sensitivity analysis. He used a small artificial pressure even if the pressure was positive to remove the tendency of particles in forming the local linear structures.

Monaghan (1992) introduced artificial viscosity for making the SPH numerical model stable. He suggested replacing the artificial viscosity with the effective viscosity term in the momentum equation by the following definition:

$$\Pi_{ij} = \frac{-2\alpha_{\Pi} C_s}{\rho_i + \rho_j} \cdot \frac{h \vec{u}_{ij} \cdot \vec{r}_{ij}}{|\vec{r}_{ij}|^2 + \eta^2} \quad \text{if } \vec{u}_{ij} \cdot \vec{r}_{ij} < 0 \quad (20)$$

Where α_{Π} is an empirical coefficient that is set to 0.1 in this study. If it is necessary to use artificial viscosity instead of effective viscosity, the viscosity term in the momentum equation should be considered as:

$$\Phi_{art} = - \sum_{j \neq i} m_j \Pi_{ij} \vec{\nabla}_i W_{ij} \quad (21)$$

Main drawback of this type of artificial viscosity is that utilizing improper coefficients can generate additional unrealistic damping throughout the whole flow domain. To limit the damping effect only to the surface boundary where the results of SPH method is not realistic due to the kernel truncation, a local surface viscosity is utilized in this study. The concept of surface viscosity was introduced by Xu (2010) and later, its workability was improved by the improvements suggested by Akbari (2017). In the modified surface viscosity method, the viscosity of surface particles is replaced with a modified viscosity as $\nu_m = \nu_E + \nu_{art-s}$ where the effective viscosity (ν_E) is the summation of laminar and turbulent viscosities and the surface artificial viscosity (ν_{art-s}) is defined as:

$$\nu_{art-s} = \alpha_s \cdot (dr_0)^2 \frac{|\vec{U}_f|}{U_{\max}} \cdot \left| \vec{\nabla} \cdot \vec{U}_f \right| \quad (22)$$

dr_0 is the initial particle spacing and U_{\max} is the absolute of the maximum particle velocities at each time step. α_s is a damping coefficient that controls the influence of the artificial viscosity and it is selected as unity as recommended by Akbari (2017). This type of surface viscosity is applicable in both ISPH and WSPH methods and in contrast to the Xu (2010)'s approach, it can be used in variety of models with different accuracies and the damping coefficient has been defined via a rigorous method. For example, in an ideal model with a free divergence velocity condition, no excess viscosity is applied to the model.

In addition, the surface viscosity is a function of local inaccuracy and therefore, it varies from a particle to another one as a function of their local inaccuracies. The workability of this modified method in damping unrealistic fluctuation at free surface boundary is investigated in this study too. It was shown by Khayyer et al. (2008) that unrealistic surface fluctuation can be decreased by use of modified gradient kernel and particle surface tracking would be improved accordingly. This modification is also used in this study to conserve the angular momentum and its efficiency in damping surface fluctuations is also investigated.

2.5. Calculation time-step

CFL, mass force and viscous force are the three criteria used for calculating the time step that varies during the simulation as:

$$\Delta t = \min \left(\alpha_t \frac{\Delta x}{U_{\max}}; \alpha_t \sqrt{\frac{h}{f_a}}; \alpha_t \frac{h}{U_{\max} + \beta_{\text{visc}} h} \right); \quad (23)$$

$$\beta_{\text{visc}} = \frac{\vec{u}_{ij} \cdot \vec{r}_{ij}}{|\vec{r}_{ij}|^2 + \eta^2}$$

f_a is the force per unit mass of the fluid that is equal to the minimum magnitude of particle accelerations and α_t is set to 0.1 in our numerical models. U_{\max} is maximum velocity of particles in ISPH method and celerity of sound (numerically 10 times the maximum velocity) in WCSPH method.

2.6. Free surface boundary

SPH integration is not accurate at the free surface boundary because the kernel function is truncated at this boundary. As a result, predicted density of surface particles via Eq. (13) is less than the actual water density. This shortcoming is utilized at each time step to detect particles located at free surface boundary. In other words, a particle i is located at the free surface boundary if its predicted density fulfills (Shao and Lo 2003):

$$\rho_i < \beta_{\text{surf}} \rho_w; \quad \beta_{\text{surf}} \cong 0.9 \quad (24)$$

After recognizing the surface particles, their pressure set to zero. In addition, a surface viscosity as introduced in Eq. (22) is applied to the surface particles to diminish any unreliable fluctuation.

2.7. Solid boundary

Different methods have been introduced for modeling solid boundary particles and several attempts have been done to make these methods more accurate. Generally, one line of fixed particles is used to model a solid boundary condition and to make density of these particles different from the truncated density of surface particles; several lines of dummy particles are

also applied parallel to the main solid boundary line to remedy the truncation error. Ferrari et al. (2009) combined different methods to get more reliable results near the wall boundary and Ferrand et al. (2012) improved modeling of solid boundaries by normalizing density of particles near this boundary. Several other methods have been introduced too; however, all of these methods can be categorized in three general groups as repulsive force methods (Monaghan 1994), fixed dummy particle methods (Shao and Lo 2003) and mirror particle methods (Colagrossi and Landrini 2003). In the first method, a repulsive force exerts on those fluid particles getting close to the solid boundary. In the second method, governing equations are solved for solid boundary particles as well as fluid particles and therefore, internal pressure will be increased when fluid particles get close to the boundary particles and prevent them from penetrating into the solid boundary. Boundary particles are fixed in this method and the pressure of outer dummy particles is set equal to the pressure of nearest wall particle to impose the homogenous Neumann boundary condition. The last method is based on considering mirror particles outside the solid boundary while their parameters are equal to the mirrored parameters of fluid particles closing to the solid boundary. Therefore, when a particle gets close to a solid boundary, it will sense its mirrored particle and pressure will be increased accordingly. Consequently, this method is comparable with the second method because the pressure term is modified by means of solving governing equations instead of imposing extra repulsive force. Therefore, the accuracy of repulsive force method in comparison with artificial particle method is investigated in this study.

Following Monaghan (1994), when distance between fluid particle and solid boundary particle get less than a defined value of r_b , in repulsive force method, an extra force (F_{ij}^R) exerts on the pair particle as:

$$\vec{F}_{ij}^R = D \left[\left(r_b / |\vec{r}_{ij}| \right)^{n1} - \left(r_b / |\vec{r}_{ij}| \right)^{n2} \right] \frac{\vec{r}_{ij}}{|\vec{r}_{ij}|} \quad ; |\vec{r}_{ij}| < r_b \quad (25)$$

Where, $n1$ and $n2$ are empirical coefficients that are suggested by Monaghan (1994) as 12.0 and 4.0, respectively and D is an empirical parameter that depends on the considered case for simulation.

3. Accuracy of WCSPH and ISPH methods

Well-known dam break flow is selected to study the performance of WCSPH and ISPH methods in modeling free surface flows. Accuracy of simulated surface profile and pressure term are investigated and the effects of different terms are discussed. Following Akbari (2017), the geometry of the problem is selected as indicated in Fig.1. The bed is wet with

depth of 0.02m and height and width of the initial water column are 0.25m and 0.28m, respectively. Total number of particles is 3280 with initial spacing as 0.005 and the total simulation time is selected as 3.2s. The simulations have been carried out on a Core2 Duo CPU T7500, 2.13 GHz and RAM 2.0 GB Laptop.

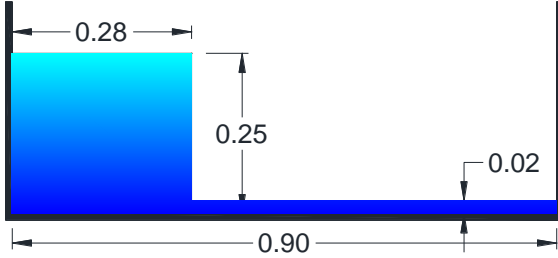


Figure 1. Initial geometry for dam break simulation

The density summation method as Eq. (13) have been used and the simulated results at $t=0.3s$ are shown in Fig. 2 for WCSPH with artificial viscosity as Eq. (21) and ISPH methods with artificial viscosity and modified surface viscosity as Eq. (21) and Eq. (22), respectively. Solid line shows the free surface profile modeled with WCSPH method. As shown in Fig. 2(a) and Fig. 2(b), the simulated surface profiles are nearly similar in both WCSPH and ISPH methods with artificial viscosity. Yet, the pressure fluctuation in WCSPH method is significantly more than fluctuation in ISPH method. For example, time series of the simulated pressures at a point on the tank floor (red point in Fig.2 at $x=0.4m, z=0.0$) are depicted in Fig. 3. Although both methods have resulted in nearly same averaged values, high fluctuations are generated in WCSPH method. Since equation of state is used to calculate the pressures of each individual particle in WCSPH method, a little inaccuracy in particle density can generate a significant local error in the pressure term. Actually imposing incompressibility in WCSPH done via pressure adjustment and during this procedure pressure accuracy sacrifices. On the other hand, a system of linear equations is solved in ISPH method to calculate the pressure and therefore, the fluctuations in ISPH results are less accordingly. It should be noted that the theoretical background of ISPH in deriving the incompressible equations is more robust than empirically introduced equation of state in WCSPH method. However, a divergence-free velocity ISPH method is implemented in this study that can suffer from conserving continuity equation during the simulation.

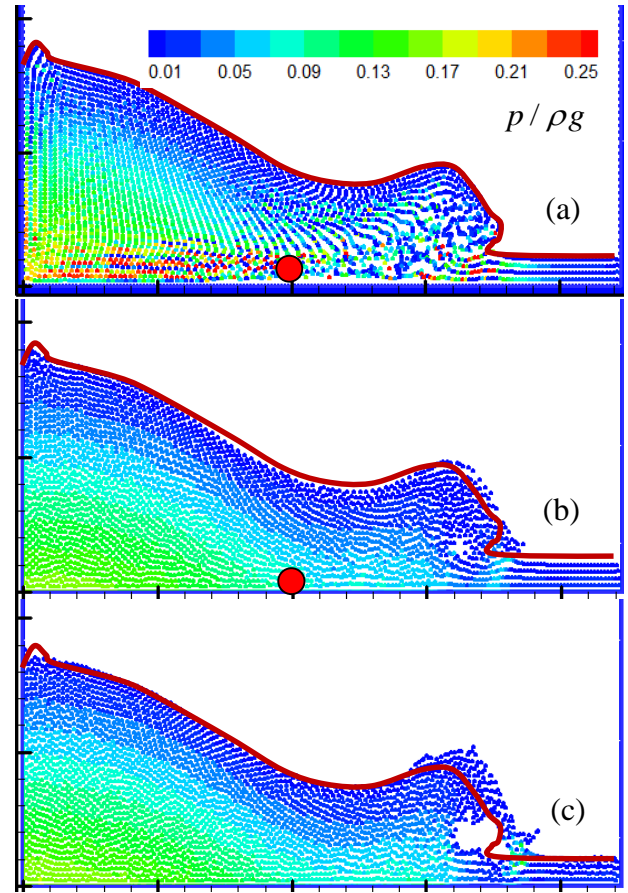


Figure 2. Simulated pressure at $t=0.3s$: a:up)WCSPH with artificial viscosity; b:middle) ISPH with artificial viscosity; c:down) ISPH with effective viscosity; (Solid line shows the surface profile in "a"), results are compatible with Akbari (2017)

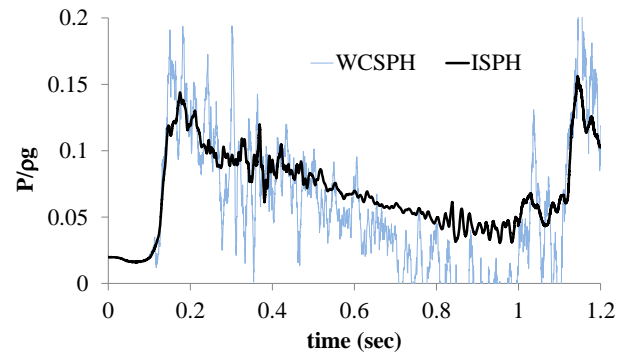


Figure 3. Time series of the simulated pressures (at $x=0.4m, z=0.0m$) using WCSPH and ISPH with same artificial viscosity

To further investigate the results, density conservation during the simulations are calculated and the error in the mean values (averaged density of all particles at each time step) are presented in Fig. 4 for both methods. It can be seen that the utilized WCSPH method is more accurate in conserving mass during the simulation than the utilized ISPH. The maximum errors in the mean density in WCSPH and ISPH methods are nearly 2% and -3%, respectively. It should be noted that local density fluctuations exist yet in WCSPH method; however variation of the mean density is smoother due to averaging between all particles. In other words, although density (and

consequently pressure) fluctuation at each particle is more in WCSPH than in ISPH, the total mass conservation is better satisfied in WCSPH model.

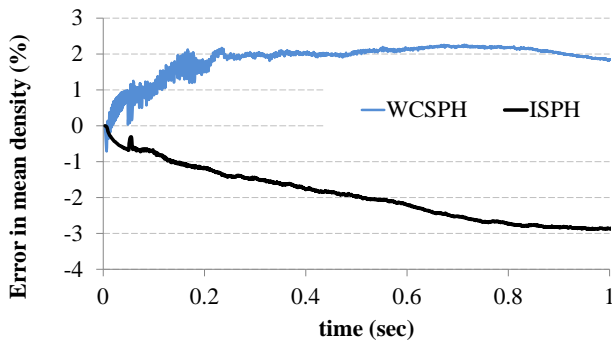


Figure 4. Error in the mean density using WCSPH and ISPH with the same artificial viscosity

As discussed by Szwed et al., (2012), mechanism of the density error in ISPH and WCSPH methods is completely different. Using an equation of state in WCSPH method generates local errors, while movement of particles with a velocity projected onto a divergence-free space with no constraint on density variation causes accumulated density errors in ISPH method. Therefore, the error of WCSPH in Fig.4 has reached to a stable point earlier than ISPH method. This drawback of ISPH can be corrected using a density invariant scheme, yet suffering from errors in velocity divergence field. Some improvements such as combining these two schemes (Xu et al., 2009) or using higher order source terms in equations (Gotoh et al., 2014) were introduced to overcome these problems of ISPH method. On the other hand, some improvements such as normalizing particle densities or using a smoothed density (Hughes and Graham, 2010) were introduced to overcome the problem of local variations in WCSPH method. There are also other modifications such as particle shifting or density normalization applicable to both methods to improve density conservation during the simulation. Since a lot of modifications have been introduced to improve ISPH and WCSPH methods, models with a similar condition are utilized in this study for making a fair comparison.

4. Stability of WCSPH and ISPH methods

Although ISPH method is shown to be more robust and more accurate than WCSPH method particularly in simulating pressure term, using a global artificial viscosity can damp the real flows as a result of the utilized artificial viscosity (α_{Π}). As mentioned before, artificial viscosity is used to stabilize the numerical solution. However, high artificial viscosity will generate unrealistic damping and inadequate empirical coefficient may affect the model accuracy (even in predicting surface profile). The importance of selecting an appropriate artificial viscosity in modeling dam break flows has been studied by Khayyer and Gotoh (2010b). Although the empirical

coefficient (α_{Π}) can be calibrated via experimental studies, laboratory data are not always available and therefore, the better solution is implementing effective viscosity instead of artificial viscosity. Considering effective viscosity, simulated pressure pattern by means of ISPH method is shown in Fig. 2(c). By comparing Fig. 2(b) with Fig. 2(c), it is clear that a sharp wave profile can be modeled more clearly by means of implementing effective viscosity rather than artificial viscosity. On the other hand, by comparing the free surface profiles, it can be concluded that an extra damping has been occurred in the case of using artificial viscosity.

In addition to the additional viscosities, the smoothing length in kernel function can affect the results and control the numerical stability of the methods. If higher (doubled) smoothing length as $h = 2.4dr_0$ is taken into account instead of $h = 1.2dr_0$, surface profile will not be as smooth as before because more particles may stick together as a result of tensile instability problem. Particle clustering during wave breaking is shown in Fig. 5(b) while there will be no problem if less smoothing length is used in simulation as Fig. 5(a). A part of the wave profile is presented in higher resolution in this figure to clarify particle clustering. Actually, when particles get closer than a specific distance (i.e. $2h/3$ in the case of using Cubic-Spline kernel), they will be affected by tensile instability problem and if higher smoothing length is utilized more particles may be surrounded making the results inaccurate while the simulation is still stable. However, the WCSPH method is not stable and the simulation diverges as presented in Fig. 6(a) if effective viscosity is used without any stabilization technique. As shown in this figure, in addition to solution divergence, tensile instability is performed even by means of $h = 1.2dr_0$ and some particles are moving as a collocation surrounded inside the kernel function. This instability does not happen in ISPH method, however, if higher smoothing length is used, more particles may stick together and make even ISPH solution unstable. Although this problem can be solved by means of tensile correction technique, WCSPH method is unstable yet because of effective viscosity as shown in Fig. 6(b). This means that particle collocation due to tensile instability can be removed by decreasing the smoothing length in both ISPH and WCSPH methods, however, WCSPH can be yet unstable and there is a need to use artificial viscosities for making this method stable. On the other hand, decreasing the smoothing length is limited and inadequate reduction can lead to insufficient contribution of neighbor particles than will result finally in divergence problems during the solution.

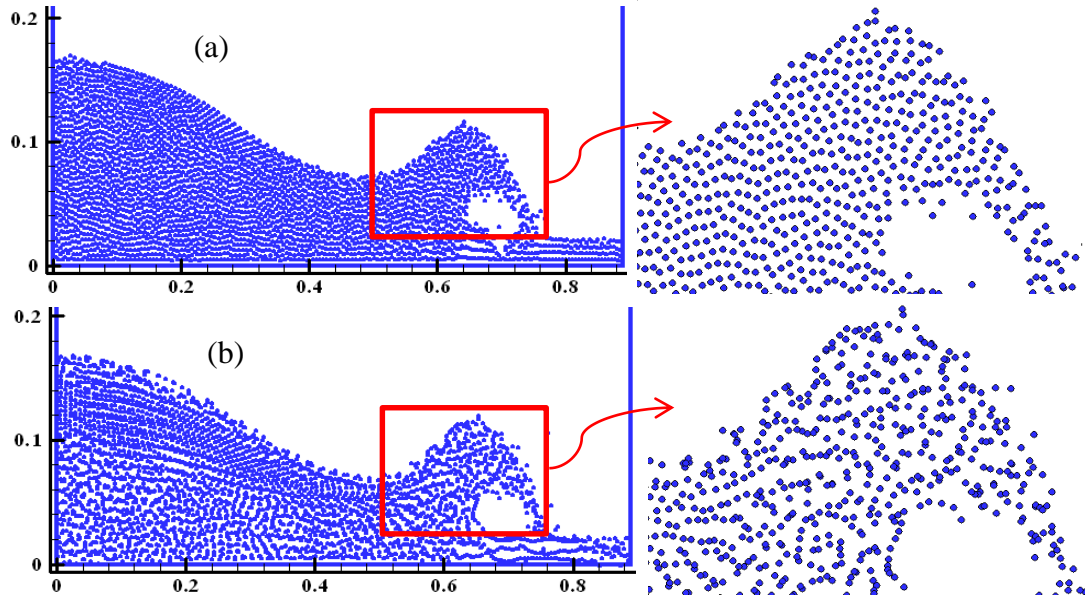


Figure 5. Particles during simulated wave breaking by ISPH method and effective viscosity at $t=0.3s$;
a:up) $h = 1.2dr_0$; b:down) $h = 2.4dr_0$

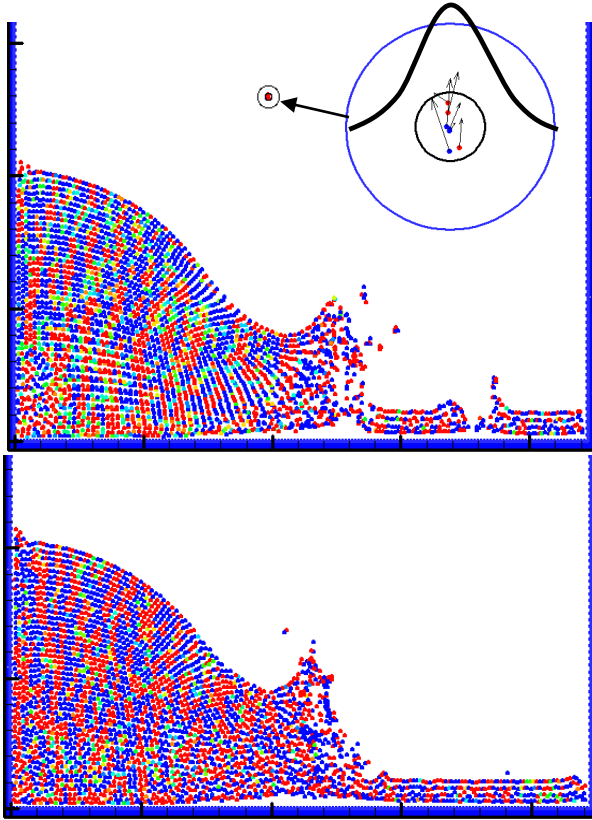


Figure 6. Simulated pressure by WCSPH method and effective viscosity at $t=0.2s$; a:up) without tensile correction; b:down) with tensile correction

5. Surface boundary and local fluctuations

According to the results, ISPH method is more stable than WCSPH method and it is also more reliable particularly in predicting pressure term. However, unreliable surface fluctuation may occur even in ISPH method. Although this problem can be solved by means of artificial viscosity as introduced by Monaghan (1992), accuracy of the results will be

decreased by artificial viscosity as declared before. An effective method in controlling unreliable surface fluctuation is implementing additional surface viscosity as introduced by Akbari (2017) via Eq. (22). The effect of imposing surface viscosity in reducing particle jumps near free surface boundary is presented in Fig. 7.

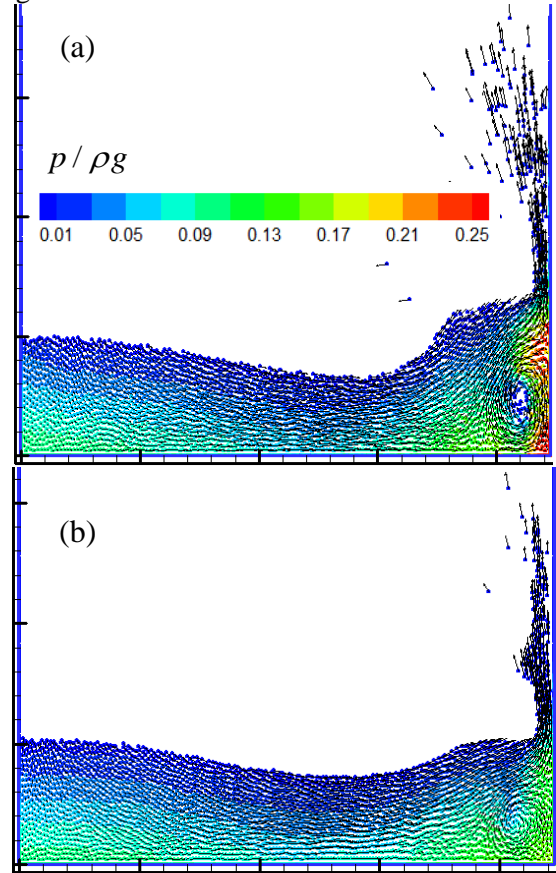


Figure 7. Simulated dam break flow by ISPH method at $t=0.5s$; a:up) non-viscous; b:down) modified surface viscosity

As shown in Fig. 7(a), if no viscosity is applied to the fluid, particles will move in a disordered condition particularly near the surface profile. However, these movements are controlled by means of imposing surface viscosity as indicated in Fig. 7(b) and a smoother surface profile has been modeled. It should be noted that utilizing very large damping coefficient can yet results in a global damping similar to the effect of imposing traditional artificial viscosities.

Khayyer et al. (2008) showed that unrealistic surface fluctuation could be decreased by means of modified gradient of kernel function. This modification is considered in this study because angular momentum is preserved by this modification. However, its efficiency in smoothing the surface profile should be studied more in comparison with the surface viscosity. Pressure contours in addition to surface particles are presented in Fig. 8 during wave breaking at $t=0.3s$.

As shown in Fig. 8(a), wave profile is straggly if neither kernel gradient modification nor surface viscosity is used and this uneven behavior will not be solved by use of kernel gradient modification as presented in Fig. 8(b). However, as shown in Fig. 8(c), a smooth wave profile can be simulated by means of surface viscosity even if no kernel modification is

utilized.

In addition, if both modified kernel gradient and surface viscosity are used, simulated wave profile will be smooth and no fluctuation will be seen in the surface profile according to Fig. 8(d). Both of these modifications shall be used in numerical modeling because surface fluctuation can be efficiently removed by means of the surface viscosity while angular momentum can be preserved via modified gradient of kernel function. Although unreliable surface fluctuation may be decreased by utilizing modified kernel gradient, the effect of the surface viscosity in controlling the surface profile is clearly more significant and the model accuracy will be conserved by this modification. It should be noted that a general damping effect can be generated by means of imposing an artificial viscosity (as was indicated in Fig. 2(b)), however, no general damping has been occurred in the case of using surface viscosity (as indicated in all the cases in Fig. 8).

It can be concluded that by means of surface viscosity, surface fluctuation will be damped and there is no need to use stabilizing methods such as artificial viscosity.

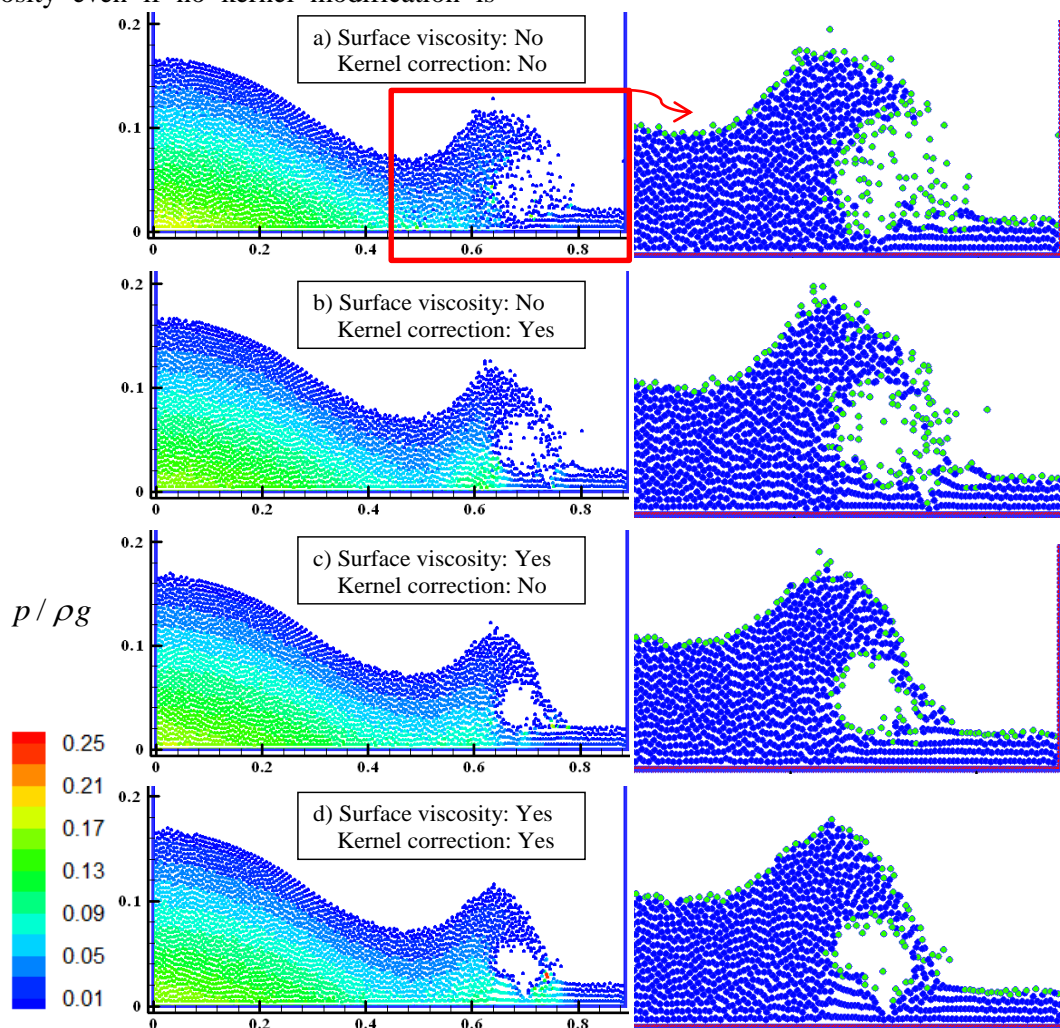


Figure 8. Simulated dam break flow by ISPH method with effective viscosity at $t=0.3s$; a) Without any modification; b) modified kernel; c) modified surface viscosity; d) modified kernel and surface viscosity

6. Solid boundary treatments

Both repulsive boundary and dummy boundary methods are used in this study to simulate dam break flow (fluid dam with 0.2m height and 0.1m width in a box with 0.3m length) by means of both WCSPH and ISPH methods. Initial particle spacing is set to 0.005m and the results of simulation by making use of dummy particle method are shown in Fig. 9 at $t=0.3s$. In this figure, ISPH result is shown with two WCSPH results based on density summation and density variation methods as Eq. (13) and Eq. (14). Similar to simulated dam break flow in the previous section, surface profile is nearly alike in the results of both ISPH and WCSPH method based on density summation method but, density variation method is not an accurate as density summation method in predicting particle positions and as shown in Fig. 9(c), particles are not uniformly distributed in the fluid domain that shows incompressibility criteria will not be satisfied completely if density summation method is used. However, dummy particle method can be utilized efficiently in modeling solid boundary both in WCSPH and ISPH methods and there is no particle penetration into solid boundary by means of this method.

Contrary to dummy particle method, there are some empirical parameters in the repulsive boundary method. The force coefficient (D) and covered distance (r_b) are two important parameters that influence on the amount of repulsive force and define those fluid particles that the repulsive force should be

exerted on. To study the efficiency of the repulsive force method, different simulation results for dam break flow is shown in Fig. 10 by considering different empirical parameters and utilizing WCSPH method. As shown before, solid boundary can be simulated properly by dummy particle method in WCSPH method that is however less accurate than ISPH method. In Fig. 10(a), empirical coefficients are set in a way to have no particle penetration to solid boundary (i.e. $r_b = 1.2dr_0$, $D = 4E-4$). If small distance is used (i.e. $r_b = 0.001$), fluid particles will not be affected by the repulsive force at a proper time because they are too close to the boundary when they receive the repulsive force and fluid particles will penetrate into solid boundary accordingly as shown in Fig. 10(b). In addition, if repulsive force does not properly set fluid particles will pass through the solid boundary as shown in Fig. 10(c). In this figure, considered repulsive force is less than what is required for preventing particles from penetrating into boundary. On the other hand, if large repulsive force is taken into account, extra force will be exerted on the fluid particles make particles reflecting back from the boundary with an unreliable velocity. Therefore, the efficiency of the repulsive boundary method depends on its empirical coefficients and unrealistic results may be obtained by means of utilizing inadequate parameters. However, this difficulty does not happen in dummy particle method because actual fluid pressure is used to satisfy boundary condition.

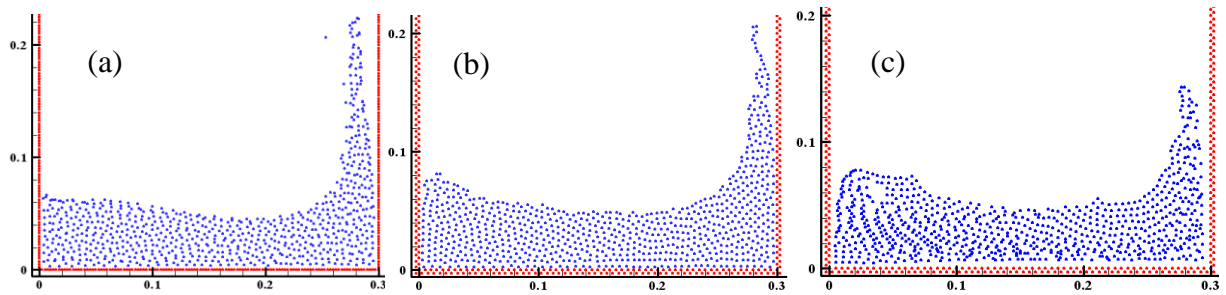


Figure 9. Simulated dam break at $t=0.3s$ with dummy particle method; a:left) ISPH; b:middle) WCSPH with density summation, c:right) WCSPH with density variation

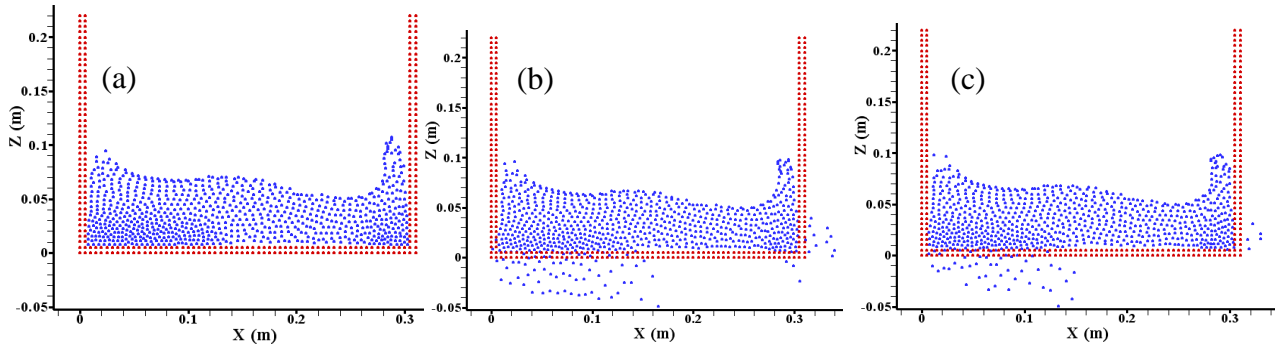


Figure 10. Simulated dam break at $t=0.3s$ with repulsive method; a:left) ($r_b=1.2dr_0$, $D=4E-4$); b:middle) small distance: ($r_b=0.001$, $D=4E-4$); c:right) small repulsive force: ($r_b=1.2dr_0$, $D=4E-6$)

7. Computational cost of ISPH vs. WSPH

Computational times of ISPH and WSPH methods are compared in modeling the dam break flow with initial condition in Fig. 1. Different special resolutions are also selected to study the computational cost of SPH methods versus number of particles. All the simulations have been performed on a Core2 Duo CPU T7500, 2.13 GHz and RAM 2.0 GB Laptop.

The required CPU times for different cases are presented in Table 1 and Fig. 11. As shown in this figure, ISPH method is more computationally efficient than WSPH for all of these cases. It should be noted that similar search algorithm (i.e. linked list method) is used for searching neighbor particles and a similar time step based on Eq. (23) is implemented. According to the transient behavior of the flow, maximum flow velocities and consequently minimum time steps change continuously during simulations. According to the time step criteria defined in Eq. (23), minimum time step will be decreased if higher velocity is observed in the simulation. For calculating the time step, speed of sound is taken into account in WSPH method while maximum flow velocity is used in ISPH method. Therefore, time step is less in WSPH method than in ISPH method.

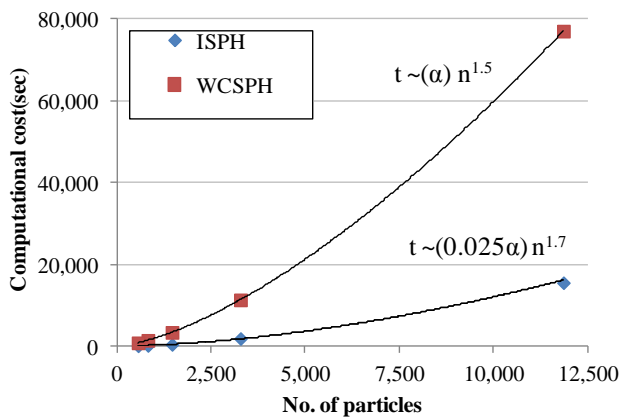


Figure 11. Computational cost of ISPH and WSPH in simulating dam break flow

Total computational cost depends on both time step increment and computational cost per time step. Time step increment is related to flow behavior as defined in Eq. (23) while computational cost per time step is

related to the implemented algorithm as well as efficient programming. According to Table 1, averaged time step in simulating the case II by ISPH method is approximately eleven times more than required time step in WSPH, however, ISPH method is only six times faster than WSPH method (11322/1867). The main reason is more computational cost per time step in ISPH method that is due to solving a system of linear equations in ISPH method. In other words, for the mentioned case (case II), computational cost per time step in ISPH method should be nearly two times (i.e. 11/6) more than what is in WSPH method to decrease the total ratio of CPU time from eleven to six. Time step can be calculated simply, yet researchers might consider various algorithms that influence on the computational cost per time step. In addition, ratio of the required computational cost of ISPH and WSPH is a function of the number of particles. Although ISPH is generally faster than WSPH, the efficiency ratio is less for larger number of particles. For example, in case I with larger number of particles, ISPH is 5 times faster than WSPH while in case II it is 6 times faster. Since WSPH programming is simpler than ISPH and most of its programming techniques exist in ISPH method too, it can be concluded that the most important issue in comparing computational cost of ISPH method against WSPH method is the utilized technique in developed ISPH model. The main distinguishing item in ISPH method is solving linear equations that are not performed in WSPH method. Since dimension of this linear system is equal to the square of particle numbers (i.e. $n_p \times n_p$), computational cost of ISPH method would be more sensitive to the number of particles in comparison with WSPH method. As shown in Fig. 11, ISPH computational cost is proportional to $n_p^{1.7}$ while the power of particle numbers is 1.5 (instead of 1.7) in case of WSPH method. Therefore, in case of utilizing very large number of particles, WSPH method can become more efficient than an ISPH method that works with a sensitive solver to the number of particles. In addition, parallel programming, as a good solution for solving large number of particles, can be applied simpler to

Table 1. Computational cost of ISPH and WSPH in simulating dam break flow

| Case | dx0 | No. of particles | Computational cost (s) | | | Averaged time step (s) | | |
|------|--------|------------------|------------------------|-------|-----------|------------------------|----------|-----------|
| | | | ISPH | WSPH | WSPH/ISPH | ISPH | WSPH | ISPH/WSPH |
| I | 0.0025 | 11861 | 15520 | 77102 | 4.97 | 1.80E-04 | 1.60E-05 | 11.25 |
| II | 0.005 | 3280 | 1867 | 11322 | 6.06 | 3.80E-04 | 3.40E-05 | 11.18 |
| III | 0.0075 | 1461 | 418 | 3372 | 8.07 | 7.30E-04 | 5.20E-05 | 14.04 |
| IV | 0.01 | 820 | 165 | 1422 | 8.62 | 9.50E-04 | 7.20E-05 | 13.19 |
| V | 0.012 | 560 | 77 | 810 | 10.52 | 1.30E-03 | 8.30E-05 | 15.66 |

WCSPH than to ISPH.

The results show that the utilized ISPH is faster than WCSPH method in solving common dam break flows. This is compatible with the results of some previous studies such as Lee et al. (2008) and Lee et al. (2010) that have reported a shorter CPU time for ISPH than WCSPH in the order of (2 to 20) times. However, these values depend on the utilized programming techniques as well as the number of particles. This is why different researchers have reported dissimilar computational costs for ISPH versus WCSPH method.

8. Conclusions

The accuracy, stability and efficiency of both WCSPH and ISPH methods are compared in this paper by means of simulating dam break flow. In addition, modeling of free surface and solid boundaries are studied to introduce an effective technique in modeling boundaries. Computational costs of these methods are then compared in solving a similar problem. It should be emphasized that each method has its individual advantage and drawbacks and a lot of modifications have been introduced to amend drawbacks. Meanwhile, original forms or similar modifications are taken into account in this study to get fair comparison results and discover intrinsic drawbacks. Based on the results:

a) Simulated free surface profile is nearly similar in both ISPH and WCSPH methods. However, simulated pressure is not accurate in WCSPH method while no unrealistic pressure fluctuation occurs in ISPH method.

b) Unrealistic fluctuation of surface particles can be removed by means of the surface viscosity while keeping the model accuracy. In simulated cases, the effect of surface viscosity in smoothing surface profile is more significant than modifying the gradient of kernel function.

The results of WCSPH method are more accurate in case of utilizing density summation method in comparison with utilizing density variation method. Although density fluctuation at each particle is more sensible in WCSPH than in ISPH method, the total mass continuity is better satisfied in original form of WCSPH method than in original form of ISPH method written based on divergence-free velocity scheme.

c) Dummy and mirror particle methods are more accurate than repulsive force method in modeling solid boundaries.

d) ISPH method is generally more stable than WCSPH method. Although artificial viscosity can be used to stabilize WCSPH method, the model accuracy will be decreased in this situation.

e) Both models will be unstable in case of utilizing small smoothing length because of insufficient number of interaction particles; however,

tensile instability may occur in addition to unreliable smoothing effect if improper large smoothing length is utilized. Therefore, smoothing length is proposed as 1.2 times of the initial particle spacing.

f) Time step and computational cost per time step are two important items in total efficiency of models. Although WCSPH is more efficient than ISPH in solving each time step (nearly twice faster in the modeled cases in this study), bigger time steps (nearly ten times based on the maximum particle velocities versus sound velocity) can be used in ISPH method. Computational cost per time step depends on the number of particles as well as the utilized solver in ISPH method. According to the simulated cases in this study, ISPH is nearly five times faster than WCSPH method, however, this conclusion would be different in case of using other solvers.

g) In comparison with WCSPH method, the computational cost of ISPH method is more sensitive to the number of particles because a system of linear equations should be solved in each step of the solution that is an important item in ISPH efficiency.

It should be noted that

Meanwhile

9. References

- 1- Akbari, H., (2017). *Simulation of wave overtopping using an improved SPH method*. Coastal Engineering. 126, 51–68.
- 2- Asai, M., Aly, A.M., Sonoda, Y., Sakai, Y. (2012). *A stabilized incompressible SPH method by relaxing the density invariant condition*. Journal of Applied Mathematics. 2012, 24 pages.
- 3- Bonet, J., Lok, T.S. (1999). *Variational and momentum preservation aspects of smooth particle hydrodynamic formulation*. Computer Methods in Applied Mechanics and Engineering. 180, 97–115.
- 4- Colagrossi, A., Landrini, M. (2003). *Numerical simulation of interfacial flows by smoothed particle hydrodynamics*. Journal of Computational Physics. 191(2), 448–475.
- 5- Dehnen W., Aly H. (2012), *Improving convergence in smoothed particle hydrodynamics simulations without pairing instability*. Monthly Notices of the Royal Astronomical Society. 000, 1-15.
- 6- Fatehi, R., Manzari, M.T. (2012). *A consistent and fast weakly compressible smoothed particle hydrodynamics with a new wall boundary condition*. International Journal for Numerical Methods in Fluids. 68, 905–921.
- 7- Ferrari, A., Dumbser M., Toro E. F., Armanini A. (2009). *A new 3D parallel SPH scheme for free surface flows*. Computers & Fluids. 38, 1203–1217.
- 8- Ferrand, M., Laurence, D., Rogers, B., Violeau, D., Kassiotis, C. (2012), *Unified semi-analytical wall boundary conditions for inviscid, laminar or turbulent flows in the meshless SPH*

- method. International Journal for Numerical Methods in Fluids. 71(4), 446–472.
- 9- Gomez-Gesteira, M., Rogers, B.D., Dalrymple, R.A., Crespo, A.J.C. (2010a). *State-of-the-art of classical SPH for free-surface flows*. Journal of Hydraulic Research. 48(Extra Issue), 6-27.
- 10- Gomez-Gesteira, M., Rogers, B.D., Violeau, D., Grassa, J.M., Crespo, A.J.C. (2010b). *Foreword: SPH for free-surface flows*. Journal of Hydraulic Research. 48(Extra Issue), 3-5.
- 11- Gotoh, H., Khayyer, A., Ikari, H., Arikawa, T., Shimosako, K. (2014). *On enhancement of Incompressible SPH method for simulation of violent sloshing flows*, Applied Ocean Research. 46, 104-115.
- 12- Gotoh, H., Khayyer, A. (2016). *Current achievements and future perspectives for projection-based particle methods with applications in ocean engineering*. J. Ocean Eng. Mar. Energy 2(3), 251–278.
- 13- Hughes, J.P., Graham, D.I. (2010). *Comparison of incompressible and weakly-compressible SPH models for free-surface water flows*. Journal of Hydraulic Research. 48, 105-117.
- 14- Khayyer, A., Gotoh, H., Shao, S.D. (2008). *Corrected Incompressible SPH method for accurate water-surface tracking in breaking waves*. Coastal Engineering. 55, 236–250.
- 15- Khayyer, A., Gotoh, H., 2010a. *A higher order Laplacian model for enhancement and stabilization of pressure calculation by the MPS method*. Appl. Ocean. Res. 32(1), 124–131.
- 16- Khayyer, A., Gotoh, H., 2010b. *On particle-based simulation of a dam break over a wet bed*. Journal of Hydraulic Research. 48(2), 238–249.
- 17- Khayyer, A., Gotoh, H., Shimizu, Y., 2017. *Comparative study on accuracy and conservation properties of two particle regularization schemes and proposal of an optimized particle shifting scheme in ISPH context*. Journal of Computational Physics. 332, 236–256.
- 18- Lee, E.S., Moulinec, C., Xu, R., Violeau, D., Laurence, D., Stansby, P. (2008). *Comparisons of weakly compressible and truly incompressible algorithms for the SPH mesh free particle method*. Journal of Computational Physics. 227, 8417–8436.
- 19- Lee, E.S., Violeau, D., Issa, R., Ploix, S. (2010). *Application of weakly compressible and truly incompressible SPH to 3-D water collapse in waterworks*. Journal of Hydraulic Research. 48, 50-60.
- 20- Monaghan, J.J. (1989). *On the problem of penetration in particle methods*. Journal of Computational Physics. 82(1), 1–15.
- 21- Monaghan, J.J. (1992). *Smoothed particle hydrodynamics*. Annual Review of Astronomy and Astrophysics. 30, 543–574.
- 22- Monaghan, J.J. (1994). *Simulating free surface flows with SPH*. Journal of Computational Physics. 110 (2), 399-406.
- 23- Monaghan, J.J., Kos, A. (1999). *Solitary waves on a Cretan beach*. Journal of Waterway, Port, Coastal, and Ocean Engineering (ASCE). 125, 145–154.
- 24- Monaghan, J.J. (2000). *SPH without a Tensile Instability*. Journal of Computational Physics. 159, 290–311.
- 25- Price, D.J. (2012). *Smoothed particle hydrodynamics and magnetohydrodynamics*. Journal of Computational Physics. 231(3), 759–794.
- 26- Rafiee, A., Cummins, Sh., Rudman, M., Thiagarajan, K. (2012). *Comparative study on the accuracy and stability of SPH schemes in simulating energetic free-surface flows*. European Journal of Mechanics - B/Fluids. 36, 1–16.
- 27- Shadloo, M.S., Zainali, A., Yildiz, M., Suleman, A. (2012). *A robust weakly compressible SPH method and its comparison with an incompressible SPH*. International Journal for Numerical Methods in Engineering. 89, 939–956.
- 28- Shao, S.D., Lo, E.Y.M. (2003). *Incompressible SPH method for simulating Newtonian and non-Newtonian flows with a free surface*. Advances in Water Resources. 26, 787–800.
- 29- Shao, S.D. (2010). *Incompressible SPH flow model for wave interactions over porous media*. Coastal Engineering. 57, 304–316.
- 30- Sun, P.N., Colagrossi, A., Marrone, S., Zhang, A.M., 2017. *The δ plus-SPH model: Simple procedures for a further improvement of the SPH scheme*. Comput. Meth. Appl. Mech. Eng. 315, 25–49.
- 31- Swegle, J., Hicks, D.L., Attaway, S.W. (1995). *Smoothed Particle Hydrodynamics stability analysis*. Journal of Computational Physics. 116, 123-134.
- 32- Szewc, K., Pozorski, J., Minier, J-P. (2012). *Analysis of the incompressibility constraint in the smoothed particle hydrodynamics method*. International Journal for Numerical Methods in Engineering. 92, 343-369.
- 33- Violeau, D., Rogers, B.D., 2016. *Smoothed particle hydrodynamics (SPH) for free-surface flows: past, present and future*, J. Hydraul. Res. 54(1), 1–26.
- 34- Xu, R., Stansby, P.K., Laurence, D. (2009). *Accuracy and stability in incompressible SPH (ISPH) based on the projection method and a new approach*. Journal of Computational Physics. 228, 6703-6725.
- 35- Xu, R. (2010). *An Improved Incompressible Smoothed Particle Hydrodynamics Method and its Application in Free-Surface Simulations*. PhD Thesis. School of Mechanical, Aerospace and Civil Engineering, University of Manchester, United Kingdom.